

Femtosecond Laser Desorption of Molecularly Adsorbed Oxygen from Pt(111)

F.-J. Kao,* D. G. Busch, D. Cohen, D. Gomes da Costa, and W. Ho

Laboratory of Atomic and Solid State Physics and Materials Science Center, Cornell University, Ithaca, New York 14853-2501

(Received 2 April 1993)

Desorption of molecularly adsorbed O₂ from Pt(111) by 620 nm femtosecond laser pulses shows a nonlinear fluence dependence of the yield and a subpicosecond response time. The measurements were carried out by means of a two-pulse correlation scheme using a pulse counting quadrupole mass spectrometer. These results can be understood with a model involving multiple reexcitations of the adsorbate by photogenerated carriers.

PACS numbers: 68.45.Da, 42.65.Re, 78.90.+t, 82.65.-i

Within the last two years, two systems have been studied by pump-probe methods with femtosecond resolution: NO/Pd(111) [1,2] and CO/Cu(111) [3]. In both these cases and O₂/Pt(111) which we present here, the desorption data are incompatible with a phonon-assisted desorption process, or with the Menzel-Gomer-Redhead (MGR) mechanism for desorption induced by electronic transition [4], which leads to minute desorption rates. In all of these three cases there is both a superlinear dependence of the yield on incident fluence and an ultrafast turn-on and turn-off time for the desorption event. For both NO/Pd(111) and CO/Cu(111), a generalization of the MGR mechanism has been introduced to describe desorption from surfaces under intense electronic excitations which effectively increases the desorption rate by allowing multiple reexcitation of the adsorbate [3,5].

Our desorption studies of O₂ from O₂/Pt(111) by irradiation with femtosecond laser pulses have been motivated by previous femtosecond time-resolved desorption experiments [1-3] and low intensity continuous wave studies of the O₂/Pt(111) [6,7]. In the case of continuous wave irradiation, there is no measurable desorption or dissociation at 620 nm, while at 310 nm, the photodesorption yield was found to depend linearly on incident light intensity [6]. In contrast, with femtosecond laser excitation, a very efficient desorption was found at both 620 and 310 nm, and the laser fluence dependence of the yield is highly nonlinear. Since adsorbed oxygen molecules also dissociate upon irradiation of laser pulses, it is not possible to redose the sample between laser shots as in NO/Pd(111) [1,2] and CO/Cu(111) [3]. In this Letter we present time resolved measurements of O₂ desorption from O₂/Pt(111) upon femtosecond excitation. This is the first time resolved desorption study in which the condition of the surface changes with each laser pulse, i.e., a nonrepetitive system.

The experiments were performed in a UHV chamber equipped with an electron energy loss spectrometer, low energy electron diffraction optics, and a quadrupole mass spectrometer. Desorbed molecules were detected by the quadrupole mass spectrometer (UTI 100C) operating in pulse counting mode. The pulse counting electronics were gated with the laser pulses to suppress background

counts. The preparation and characterization of the single crystal Pt(111) were carried out using standard procedures [6]. The sample was held at a base temperature of 80 K, and was dosed by a microcapillary array with ¹⁸O₂ to saturation coverage, approximately 0.44 monolayer (ML, 1 ML = 1.49 × 10¹⁵ cm⁻²); the oxygen isotope ¹⁸O₂ was used to further minimize the background. At 80 K molecular oxygen is known to adsorb on Pt(111) as two different chemisorbed species, occupying a bridge site and an atop site which are characterized by different O-O stretch frequencies [8-10].

Desorption was induced by the output of an amplified colliding-pulse mode-locked laser operating at 10 Hz, 620 nm. Autocorrelation of the amplified laser pulse on the sample surface typically gave a pulse width (FWHM) of 150-180 fs. For 310 nm desorption, the amplified fundamental was doubled in a β barium borate (BBO) crystal. The laser beam entered and exited the UHV chamber at 28° from the sample surface normal in the desorption measurement. The 620 nm beam was collimated on the sample to form a spot size of 2 mm². The desorption correlation measurements were performed using two orthogonally polarized pulses spatially overlapping on the crystal to avoid interference. The intensity ratio of these two incident pulses was 1.3, so that the absorbed fluence was approximately the same for both pulses considering the polarization dependence of the absorptivity. The delay between these two pulses was controlled by modifying the optical path lengths with a stepping motor.

If it is assumed that the photodesorbed O₂ signal due to the *i*th laser pulse *N_i* is proportional to the change of coverage Δ*θ_i*, and this change is proportional to the coverage *θ_i*, one then has

$$N_i \propto \Delta\theta_i = \theta_i f(F_i), \quad (1)$$

where *f(F_i)* is a general functional dependence of the photoyield on fluence. In the low intensity cw limit, *f(F_i)* is simply σ*F_i* and Eq. (1) can be integrated to yield *θ_i* = *θ₀* e^{-σ∑_{j=1}ⁱ F_j}, where σ is the photodesorption cross section, *θ₀* is the initial coverage, and the summation is from the first to the *i*th pulse. In the case of a nonlinear dependence of the photoyield on fluence, *f(F_i)* = β*F_i^p*, *θ_i* can again be obtained by integrating Eq. (1),

$$\theta_i = \theta_{0e}^{-\beta \sum_{j=1}^i F_j^P}, \quad (2)$$

where P is the exponent of the power law and β is a scaling constant. The effective cross section is defined as

$$\sigma_{\text{eff}} = \frac{\beta \sum_j F_j^P}{\sum_j F_j}. \quad (3)$$

Since $N_i \propto \theta_i f(F_i)$, the raw data is simultaneously fit to a power law and a decaying coverage. A typical decay curve for the O_2 desorption signal is shown in Fig. 1, where an effective cross section of $1.6 \times 10^{-17} \text{ cm}^2$ and a power law exponent of 6.1 are obtained from the best fit.

The thermal desorption peak temperature is observed not to shift as the coverage increases, suggesting that the bonding between O_2 and Pt(111) does not vary appreciably with coverage [11]. It has also been found that only a small percentage of O_2 on Pt(111) dissociate with femtosecond laser pulses at 620 nm [12]. The good fit of the data in Fig. 1 by a single exponential decay for signal clearly above the background (initial dozen data points) indicates that the desorption can be accurately described by a single cross section. These results justify the use of

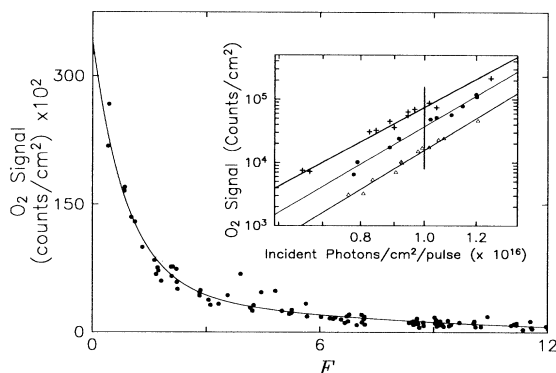


FIG. 1. $^{18}\text{O}_2$ desorption signal induced by two correlated 620 nm fs pulses from $\text{O}_2/\text{Pt}(111)$ with 750 fs delay time. Each point represents normalized desorption counts per illuminated area. To account for signal variations due to pulse-to-pulse fluctuations of the laser pulses, the counts are normalized to the P th power of the corresponding pulse fluence and plotted against effective fluence F , where $F = \beta \sum_{j=1}^i F_j^P$. The average incident pulse fluence is 3 mJ/cm^2 . The solid line is the best fit to the sum of two exponential decays with the slower decay fitting the low intensity tail which merges into the background, while the dominant initial decay yields an effective cross section of $1.6 \times 10^{-17} \text{ cm}^2$. Inset: Desorption counts vs incident pulse fluence for time delays of 0 fs (+), 750 fs (●), and 3.3 ps (Δ). The data for each time delay are from a single depletion curve, e.g., the data for the 750 fs (●) in the main part and the inset are from the same depletion run. Each symbol represents counts per pulse normalized to the decaying desorption signal, as illustrated by the solid curve in the main part of the figure. Only the first dozen data points of the signal decay are used in the analysis since the fluctuations start to become comparable to the background.

Eq. (1) in the present analysis.

We have measured the desorption yield to be proportional to the power of 5.6 ± 0.7 of the laser fluence at 620 nm in the 3 mJ/cm^2 incident fluence regime and to the power of 3.0 ± 0.5 at 310 nm in the 2 mJ/cm^2 incident fluence regime. Taking into account the dependence of reflectivity on wavelength, the absorbed fluence is approximately 1 mJ/cm^2 for these two wavelengths, leading to very similar desorption yields within the desorption model [1-3]. This indicates that a different mechanism is responsible for desorption, compared to the low intensity (cw) regime where 620 nm photons are ineffective in causing desorption, with desorption cross section $\sigma < 10^{-22} \text{ cm}^2$ [6].

In Fig. 2, the desorption signal is plotted as a function of delay time between the two pulses at 620 nm. Because of the nonlinear fluence dependence, an enhancement occurs for short delay times. The FWHM of this two-pulse correlation feature is approximately 1.2 ps. Since this number is much larger than the pulse width of 150 to 180 fs (determined by surface second harmonic generation on the sample), it is a measure of the cooling time of the hot substrate electrons which determines the time during which desorption can occur, but not the relaxation time of the adsorbed molecule. A fresh spot on the substrate is used to obtain a complete depletion curve due to desorption, as shown in Fig. 1. From these data, a series of curves such as those shown in the inset of Fig. 1 are obtained. The data points in Fig. 2 are plotted for a fixed incident fluence of different delays, as indicated by the vertical line in Fig. 1, inset. The enhancement of the O_2 yield at 0 fs time delay relative to longer time delays is not as high as expected from the measured fluence dependence of the desorption yield. This suggests that the two pulses may cause a nonlinear yield enhancement even for delay times much longer than 1 ps [2], as demonstrated

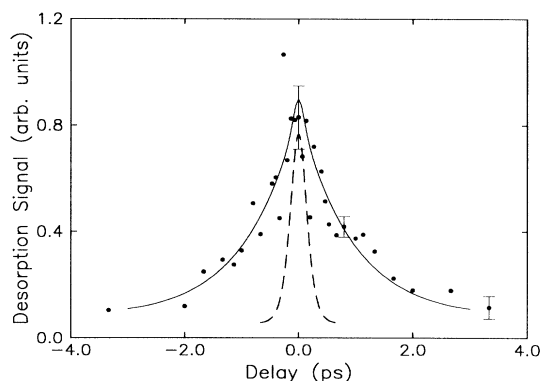


FIG. 2. Two-pulse correlation of the desorption yield as a function of pulse delay τ between two pulses, which is plotted along the solid line at fluence $1 \times 10^{16} \text{ photons/cm}^2$ for different delays, as shown in the inset of Fig. 1. The dashed curve represents the autocorrelation of the laser pulses. The solid curve is the best fit of the model to the data, with $E_{\text{th}} = 0.4 \text{ eV}$.

in the case of $O_2/Pd(111)$ [13].

Photodesorption of O_2 from $Pt(111)$ under cw light irradiation has been attributed to an electronic excitation of the adsorbate-substrate complex with the desorption induced by electronic transitions (DIET) model [6,7]. Desorption and dissociation of adsorbed O_2 molecules when irradiated by 2.3 to 5.2 eV photons are attributed to electronic transitions from below the Fermi level to π_b^* or $3\sigma_u^*$ molecular orbitals. However, the enhanced cross section and the nonlinear fluence dependence of the desorption yield obtained in femtosecond desorption suggest that under these conditions the mechanism is different from DIET. The ultrafast turn-on and turn-off times rule out slow processes, such as thermal desorption and any thermally assisted mechanism [1-3]. A direct nonresonant multiphoton electronic transition cannot account for the large observed cross section. In such a mechanism, the correlation signal shown in Fig. 2 should follow the laser intensity $I(t)$ raised to the 5.6th power, becoming narrower than the autocorrelation width of the laser pulses, in sharp contrast to the observed width.

A generalization of the MGR mechanism, "desorption induced by multiple electronic transitions" (DIMET) was proposed to account for femtosecond laser desorption [1-3,5]. In the simple DIET model, the excited adsorbate either desorbs or returns to the ground state depending on how long the adsorbate stays on the excited potential energy surface (PES), while in DIMET the adsorbate can be electronically excited repeatedly. When multiple excitation-deexcitation cycles occur within the relaxation time of the adsorbate-substrate vibration, the overall time spent in the excited PES increases and the molecules are pumped to higher vibrational energies. Such multiple excitation-deexcitation cycles also lead to a thermal-like distribution in vibrational energy [1]. Within this mechanism, the superlinear fluence dependence of the yield and the enhancement of the cross section for O_2 desorption by femtosecond pulses can be explained. The source of excitation could be nascent photoexcited electrons or "hot" electrons thermalized with each other but not with the crystal lattice.

It has been demonstrated that an intense femtosecond laser pulse induces nonequilibrium electron heating in a metal [14-18] and the resulting heat transport can be modeled by a set of coupled differential equations [19]. In the case of $NO/Pd(111)$ [2], the desorption yields of NO in two-pulse correlation measurements were compared with an Arrhenius expression employing the peak electronic temperature and an adjusted activation energy. In this way, both the response time of the two-pulse correlation and the nonlinear fluence dependence of the yield can be explained.

Similarly, in the case of $CO/Cu(111)$ [3], electrons with energy higher than a certain threshold (~ 0.5 eV above the Fermi level) were assumed to couple to adsorbed CO and induce desorption. Multiple excitations induced by these energetic electrons are believed to pump

the CO molecules to higher vibrational energies and lead to enhanced desorption. The hot electrons lose their excess energy to the lattice on a time scale of several picoseconds. For low energy electrons ($|E - E_F| < 0.3$ eV), deviations from a Fermi-Dirac distribution are possible for time delays exceeding 1 ps [20]. However, these electrons are not expected to be energetic enough to couple to the excited electronic states of the adsorbate.

The same model is used here to calculate the electronic temperature on $Pt(111)$. The electron temperature profiles for pulse delay times $\tau = 0, 750$ fs, and 3.3 ps are displayed in Fig. 3(a), and the peak T_e reached in this study is around 1500 K. Two approaches are taken to model the desorption yield obtained in two-pulse correlation. The first assumes that the yield is proportional to the α th power of the density of electrons above a threshold energy, E_{th} [3].

$$Y \sim n(t)^\alpha, \quad \alpha \geq 1, \quad (4)$$

$$n(t) = \int_{E_{th}}^{\infty} f[E, T_e(t)] g(E) dE, \quad (5)$$

where $f[E, T_e(t)]$ is the Fermi-Dirac distribution function, $g(E)$ is the density of states (taken here to be free-electron-like). Because of the distribution function $f[E, T_e(t)]$, the contribution to the desorption from electronic levels too high above E_F (several eV) can be ignored when compared with that from electronic levels closer to E_F . For $O_2/Pt(111)$, the most likely transition is excitation to π_b^* , which is approximately 0.6 eV above E_F [6]. The yield at a particular time delay is calculated by integrating $n(t)$ over the corresponding temperature profile. As a first approximation, α is chosen to be 1.

The other approach assumes that the yield takes the Arrhenius form [1,2],

$$Y \sim e^{-E_a/kT_e}, \quad (6)$$

where E_a is the activation energy. This is expected if the molecule-substrate vibration equilibrates with the hot electrons on a time scale that is fast compared to the electronic cooling [21]. The yield at a particular time delay is also calculated by integrating e^{-E_a/kT_e} over the corresponding temperature profile. An activation energy of 0.4 eV is used to best fit the calculated correlation trace with the experimental data, as shown in Fig. 2, which is very close to the binding energy of O_2 on platinum (0.38 eV) obtained from thermal desorption spectroscopy. E_a and E_{th} determine both the yield and the FWHM of the correlation trace. It can be shown that when E_{th} is chosen to be $E_F + E_a$ these two approaches generate similar two-pulse correlation traces, since $n(t)$ can be approximated by $Ae^{-(E_{th} - E_F)/kT_e}$ when $(E_{th} - E_F)/kT_e$ is much greater than 1, where A is the scaling constant. Results from the first approach are plotted in Fig. 3(b).

In the DIMET model, the nonlinearity can be understood in terms of the dependence of the electronic temperature, T_e , on the incident pulse fluence. The power-law exponent, P , for the dependence of the yield, Y , on

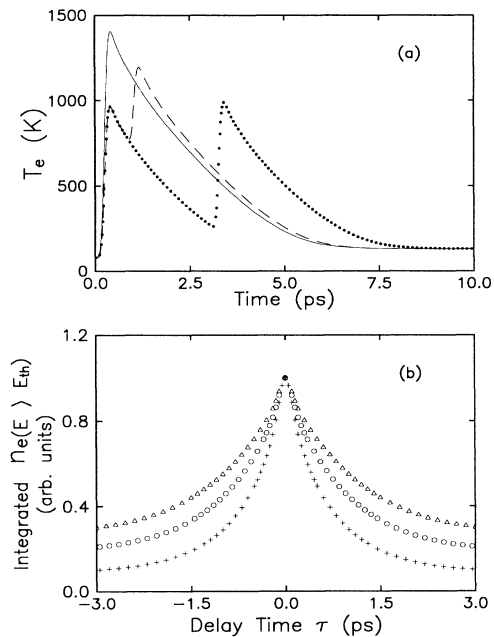


FIG. 3. (a) Calculated electronic temperature profiles from the coupled diffusion equations at 0 fs (solid curve), 750 fs (dashed curve), and 3.3 ps (dotted curve) time delays. (b) Calculated two-pulse correlation signals from the density of electrons above threshold energy, $E > E_{th}$: $E_{th} = 0.3$ eV (Δ); $E_{th} = 0.4$ eV (O); $E_{th} = 0.6$ eV ($+$).

the fluence, F , is defined as

$$P = \frac{\Delta \log(Y)}{\Delta \log(F)}, \quad (7)$$

which is calculated to be 2.7 at fluence of 3 mJ/cm^2 for an activation energy of 0.4 eV. The higher experimental value of 5.6 is attributed to the superlinear dependence of the yield on the density of hot electrons, i.e., $\alpha > 1$ [1,3].

In desorption and reaction experiments with arc lamps, nascent electrons are involved importantly in the DIET process [6], while thermalized electrons are believed to cause the DIMET process for 620 nm fs excitation [1,3]. The excitation induced by the 310 nm femtosecond pulses has a fluence dependence intermediate between nascent electrons and thermalized electrons. Since the optical skin depths [22] and the absorbed fluence used in this study for both wavelengths are very close, the change of the power-law exponents cannot be simply attributed to differences in the electronic temperature profiles. The dependence of the power-law exponent on the incident light wavelength suggests that the contribution from nascent electrons cannot be ignored; the 310 nm laser pulses generate more energetic nascent electrons.

Support of this research by the Office of Naval Re-

search under Grant No. N00014-90-J-1214 and the Department of Energy under Grant No. DE-FG02-91-ER14205 is gratefully acknowledged. In addition, the authors would like to thank F. M. Zimmermann for invaluable contributions and J. A. Misewich for illuminating discussions.

*Present address: Physics Department, National Sun Yat-Sen University, Kaohsiung, Taiwan, Republic of China.

- [1] J. A. Prybyla *et al.*, Phys. Rev. Lett. **64**, 1537 (1990).
- [2] F. Budde *et al.*, Phys. Rev. Lett. **66**, 3024 (1991).
- [3] J. A. Prybyla, H. W. K. Tom, and G. D. Aumiller, Phys. Rev. Lett. **68**, 503 (1992).
- [4] D. Menzel and R. Gomer, J. Chem. Phys. **41**, 3311 (1964); P. A. Redhead, Can. J. Phys. **42**, 886 (1964).
- [5] J. A. Misewich, T. F. Heinz, and D. M. Newns, Phys. Rev. Lett. **68**, 3737 (1992).
- [6] W. D. Mieher and W. Ho, J. Chem. Phys. **91**, 2755 (1989); (to be published).
- [7] X.-Y. Zhu *et al.*, J. Chem. Phys. **91**, 5011 (1989).
- [8] N. R. Avery, Chem. Phys. Lett. **96**, 371 (1983).
- [9] J. L. Gland, B. A. Sexton, and G. B. Fisher, Surf. Sci. **95**, 587 (1980).
- [10] H. Steininger, S. Lehwald, and H. Ibach, Surf. Sci. **123**, 1 (1982).
- [11] J. L. Gland, Surf. Sci. **93**, 487 (1980).
- [12] F.-J. Kao *et al.*, Phys. Rev. Lett. **70**, 4098 (1993).
- [13] A. Kalamarides *et al.*, QELS'93 Technical Digest, QWA4, p. 129.
- [14] P. B. Corkum, F. Brunel, and N. K. Sherman, Phys. Rev. Lett. **61**, 2886 (1988).
- [15] R. W. Schoenlein *et al.*, Phys. Rev. Lett. **58**, 1680 (1987).
- [16] S. D. Brorson, J. G. Fujimoto, and E. P. Ippen, Phys. Rev. Lett. **59**, 1962 (1987).
- [17] J. G. Fujimoto, J. M. Liu, and E. P. Ippen, Phys. Rev. Lett. **53**, 1837 (1984).
- [18] H. E. Elsayed-Ali *et al.*, Phys. Rev. Lett. **58**, 1212 (1987).
- [19] S. I. Anisimov, B. L. Kapeliovich, and T. L. Perel'man, Zh. Eksp. Teor. Fiz. **66**, 776 (1974) [Sov. Phys. JETP **39**, 375 (1975)].
- [20] W. S. Fann *et al.*, Phys. Rev. Lett. **68**, 2834 (1992).
- [21] D. M. Newns, T. F. Heinz, and J. A. Misewich, Prog. Theor. Phys. **106**, 411 (1991).
- [22] E. D. Palik, *Handbook of Optical Constants of Solids* (Academic Press, Orlando, 1985).
- [23] R. C. Weast, *Handbook of Chemistry and Physics* (CRC Press, Boca Raton, 1992), 72nd ed.
- [24] The peak substrate electronic temperature T_e for CO/Cu(111) seems too low, since the absorbed fluence is close to that of NO/Pd(111) while the coefficient of electron specific heat γ of copper is an order of magnitude smaller than that of palladium.